JOURNAL OF VIROLOGY, May 1981, p. 661-670
0022-538X/81/050661-10$02.00/0

Vol. 38, No. 2

Comparative Analysis of RNA Genomes of Mouse Hepatitis Viruses

MICHAEL M. C. LAI* AND STEPHEN A. STOHLMAN

Departments of Microbiology and Neurology, University of Southern California School of Medicine, Los Angeles, California 90033

Received 16 December 1980/Accepted 18 February 1981

The RNA genomes of various murine hepatitis virus (MHV) strains were studied by T_1-oligonucleotide fingerprinting analysis with regard to their structure and sequence relationship. It was found that the MHV particles contained only positive-stranded 60S RNA which had a "cap" structure at its 5' end. No negative-stranded RNA was found. It was also shown that most of the MHV strains had diverged quite extensively in their genetic sequences. However, MHV-3, a hepatotropic strain, and A59, a nonpathogenic strain, were found to have very similar oligonucleotide fingerprinting patterns. Yet, each of them contained two to four specific oligonucleotides. The MHV-3-specific oligonucleotides were conserved in almost all of the hepatotropic MHV strains studied. In contrast, two of the A59-specific oligonucleotides were absent from the genomes of all hepatotropic strains. These findings suggest that these unique oligonucleotides might be localized at the genetic region(s) associated with viral pathogenicity or other biological properties of the virus. Comparison of viral structural proteins also suggests that MHV-3 and A59 are more closely related than other MHV strains. The significance of these findings is discussed.

Murine hepatitis viruses (MHVs) are members of the family Coronaviridae, which includes viruses infecting a variety of animals (17, 28). Structurally, MHV is an enveloped virus which contains helical nucleocapsid (18). The viral genome consists of single-stranded 60S RNA with a molecular weight of 5.4×10^6 (15, 31). Although it has been suggested that the 60S MHV RNA is a positive-stranded RNA because it contains polyadenylic acid [poly(A)] sequences and is infectious (15, 31), the inclusion of negative-stranded RNA in MHV has not been ruled out. This possibility is particularly interesting because 60 to 70% of the 60S MHV RNA does not contain poly(A) (15) and because all of the known enveloped, helical RNA viruses contain negative-stranded RNA genomes.

MHVs have been isolated from many laboratory strains of mice (4, 17). They induce a variety of diseases in experimental animals. Although most MHV strains cause hepatitis of differing severity, a few strains are able to induce acute and chronic neurological diseases. For instance, strain JHM induces both acute and chronic demyelinating encephalomyelitis (10, 24, 33), and strain MHV-3, which causes hepatitis in most strains of mice, induces chronic choroidoependymitis and meningitis in some other strains of mice (29). Still another strain, A59, has very low pathogenicity (19). The diversity in the disease potential of different members of the MHV group offers an interesting system for the study of the mechanism of viral pathogenicity.

In this report, we have characterized the RNA genomes of various strains of MHV by oligonucleotide fingerprinting. We found that MHV contained only positive-stranded RNA. We have also compared different MHV strains of varying pathogenicity and identified some variations in their genetic sequences which might be associated with their different biological and pathogenic properties.

MATERIALS AND METHODS

Viruses and cells. Strains MHV-1, MHV-3, and MHV-S, which were originally isolated from mice dying of acute hepatitis (7, 9, 21), were obtained from Michael Collins, Microbiological Associates, Bethesda, Md. These strains have been shown in several laboratories to cause hepatitis of varying severity in different strains of mice (16, 27, 34). Strain MHV-2, which causes severe hepatitis in mice (26), was obtained from K. Fujiwara, Univeristy of Tokyo, Tokyo, Japan. Strain A59, which has very low virulence (19), was obtained from J. Robb, University of California, San Diego, La Jolla, Calif. Strain JHM was originally isolated from a mouse with hind leg paralysis and demyelination (2, 5). The DL strain, a large-plaque variant of JHM, was used in this study (15).

All the viruses were plaque purified three times on DBT cells (12) before use.

Growth and radiolabeling of viruses. Viruses

were propagated in 15-cm dishes containing monolayers of DBT cells, with the exception of strain MHV-3, which was also propagated in monolayers of L-2 cells (25). Viruses were adsorbed to cells at multiplicity of infection of 1 to 5 for 60 min at 37°C. For strain JHM, multiplicity of infection of 0.1 to 1.0 was used. The following schedule, with minor variations, was used for all viruses. After adsorption, the inoculum was removed, and 25 ml of Dulbecco modified minimal essential medium containing 1% heat-inactivated (56°C for 30 min) fetal calf serum was added. After 4 h, the medium was removed and replaced with phosphate-free Dulbecco modified minimal essential medium containing 1% dialyzed fetal calf serum and 200 μCi of $^{32}P_i$ (ICN Pharmaceuticals) per ml. Supernatants were collected 14 h postinfection.

Purification of viruses. Supernatants were cleared of cell debris at 15,000 × *g* for 30 min at 4°C, and the virus was then pelleted from the supernatants through 20% sucrose prepared in TEM buffer (0.05 M Tris-malate–0.1 M NaCl–0.01 M EDTA [pH 6.2]) at 25,000 rpm for 2.5 h in an SW27 rotor at 4°C. The pellets were resuspended in TEM and centrifuged at 40,000 rpm in an SW41 rotor for 2 h in a linear 20 to 42% sucrose gradient prepared in TEM. Fractions were collected from the bottom of the centrifuge tube, and those containing the peak radioactivity (density, ca. 1.18 g/ml) were pooled.

Extraction of viral RNA. Viral RNA was extracted from purified virus by a modification of published procedures (15). The virus was incubated with proteinase K (50 μg/ml) in the presence of 0.5% sodium dodecyl sulfate at 37°C for 20 min. The RNA was then extracted once with phenol-chloroform (1:1) and then with phenol alone. The RNA was then precipitated with 3 volumes of ethanol at −20°C overnight, pelleted by centrifugation at 20,000 × *g* for 15 min, and then sedimented in an SW50.1 rotor at 50,000 rpm for 60 min in a 10 to 25% sucrose gradient made up in NTE buffer (0.01 M Tris-hydrochloride [pH 7.4]–0.1 M NaCl–0.001 M EDTA). The MHV RNA prepared by this procedure of viral growth, purification, and RNA extraction consisted only of 60S RNA. No small 4S RNA was observed as reported previously (15). Thus, the 4S RNA was probably an artifact of the growth conditions.

Oligonucleotide fingerprinting. The ^{32}P-labeled 60S RNA was exhaustively digested with RNase T_1 and analyzed by two-dimensional polyacrylamide gel electrophoresis by a modification of the procedure of deWachter and Fiers (6). The first dimension was performed on 9.7% polyacrylamide gel slabs (30 by 10 by 0.15 cm) at pH 3.3 and 700 V for 4 h. The second dimension was performed on 22% polyacrylamide gel slabs (40 by 35 by 0.075 cm) at pH 8.0 and 650 V for 16 h. After electrophoresis, the gel was wrapped with Saran Wrap and exposed to Kodak BB-1 film with an intensifying screen at 4°C for appropriate lengths of time.

Detection of the 5′ "cap" structure. The ^{32}P-labeled 60S RNA was digested with RNases A, T_1, and T_2 according to published procedures (30). Digestion was done in 10 μl of a solution containing 0.04 M ammonium acetate (pH 4.4), 1 mM EDTA, 20 μg of RNase A per ml, 150 U of RNase T_1 per ml, and 5 U of RNase T_2 per ml at 37°C for 2 h. After digestion, the reaction mixture was spotted on DEAE-cellulose paper and electrophoresed at pH 3.5 (pyridine-acetate buffer) until a xylene cyanol FF blue marker had migrated 10 cm from the origin. The dried paper was then exposed to Kodak BB-5 film for appropriate periods of time. Because less than 1% of the ^{32}P-labeled radioisotope was present in the cap structure, the lower part of the DEAE paper was exposed to the film in the presence of an intensifying screen. The cap structure of Rous sarcoma virus RNA was used as a marker.

Polyacrylamide gel electrophoresis of viral proteins. Sodium dodecyl sulfate-polyacrylamide slab gel electrophoresis was performed as described by Laemmli (14). The ^3H-amino acid-labeled virus was pelleted by sedimenting at 100,000 × *g* for 1 h and then suspended in sample buffer (14). After heating at 80°C for 3 min, the sample was electrophoresed in a 6 to 18% linear gradient of polyacrylamide gel slabs (12 by 14 by 0.15 cm) at 10 mA for approximately 4 h. Alternatively, the electrophoresis was performed in 10% polyacrylamide gel slabs (16 by 22 by 0.3 cm) at 5 mA for 16 h. After electrophoresis, the gel slabs were treated for fluorography with (2,5-diphenyloxazole) (3), dried, and then exposed to Kodak RP film for various lengths of time.

RESULTS

Oligonucleotide fingerprinting of poly(A)-containing and poly(A)-lacking MHV RNA. It has been shown previously that 30 to 40% of the 60S RNA genomes of MHV contain poly(A) sequences, and, therefore, are positive-stranded RNA (15, 31). It was not clear, however, whether the virion also contained negative-stranded RNA. If this was the case, then the poly(A)-lacking RNA would be expected to have genetic sequences different from those of the poly(A)-containing RNA fraction. To check this possibility, we fractionated ^{32}P-labeled 60S RNA from strain JHM by oligodeoxythymidylic acid-cellulose or polyuridylic acid-Sepharose chromatography. A total of 30% of the 60S RNA bound to these columns and was designated poly(A)+ RNA. The remainder of the RNA was designated poly(A)−. These two RNA fractions were then digested with RNase T_1 and analyzed by two-dimensional polyacrylamide gel electrophoresis. The poly(A)+ fraction contained a poly(A) spot (not shown on these fingerprints), whereas the poly(A)− fraction did not, indicating that the separation of these two RNA fractions was complete. As shown in Fig. 1, their T_1-oligonucleotide fingerprinting patterns were extremely similar, suggesting that these two fractions probably have very similar, if not identical, genetic sequences. However, there are some differences in the relative molar ratios of the oligonucleotides in the fingerprints of these two RNA fractions. The poly(A)+ RNA contained several spots (indicated by triangles in Fig. 1)

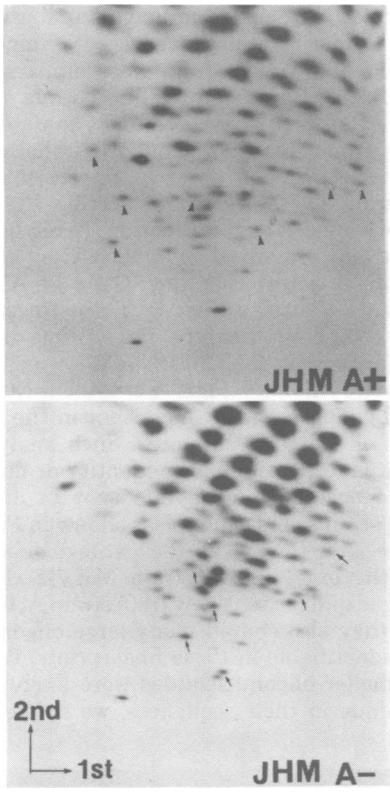

FIG. 1. *Oligonucleotide fingerprints of poly(A)+ and poly(A)- JHM RNA. The ^{32}P-labeled JHM RNA was separated into poly(A)+ (A+) and poly(A)- (A-) fractions by oligodeoxythymidylic acid-cellulose column chromatography according to published procedures (1). These two RNA fractions were digested with RNase T_1 and separated by two-dimensional polyacrylamide gel electrophoresis. The spots denoted by triangles are those that were enriched in poly(A)+ fractions, and the spots denoted by arrows are those that were enriched in poly(A)- fractions.*

which were either missing or present at relatively lower concentrations in the poly(A)- fractions. Ordering of these spots on the RNA genome showed that these spots were all localized at the 3' end (unpublished observation). On the other hand, the poly(A)- fractions also contained a few spots (indicated by arrows in Fig. 1) which were present at lower concentrations in the poly(A)+ fractions. Ordering of these oligonucleotides revealed that these spots were localized at the extreme 5' end of the RNA genome (unpublished observation). Therefore, these results suggest that both RNAs are genetically identical and that the poly(A)- RNA probably represents the degradation product of the poly(A)+ RNA fractions. It has previously been shown that MHV RNA is relatively unstable and could be degraded easily by prolonged incubation of virus in the culture medium (15). These data thus ruled out the presence of large amounts of negative-stranded RNA in the MHV virion. A similar conclusion was reached with the genomic RNA of strain A59 (data not shown).

5' cap structure of MHV RNA. To further understand the structure of the 60S MHV RNA, we studied it for the presence of the cap structure at the 5' end of the genome (8, 22). The ^{32}P-labeled 60S MHV RNA was digested with a mixture of RNases A, T_1, and T_2 and then electrophoresed on DEAE-cellulose paper at pH 3.5. Under these conditions, the RNA was digested predominantly into mononucleotides, with a small amount of dinucleotides. The cap structure was preserved and had a characteristic electrophoretic mobility near the origin (22, 30). As shown in Fig. 2, the MHV RNA contained a cap structure which had an electrophoretic mobility similar to that of the cap structure in Rous sarcoma virus RNA (13, 30). Furthermore, we separated poly(A)+ fraction from poly(A)- fractions of the 60S MHV RNA and performed

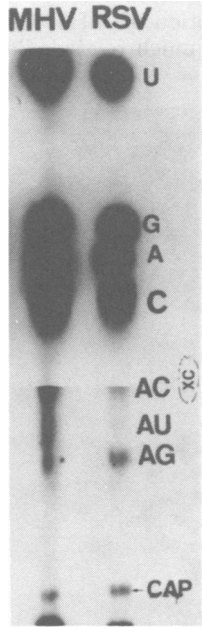

FIG. 2. *Electrophoretic separation of RNA digests of MHV. The ^{32}P-labeled A59 RNA was digested with RNases A, T_1, and T_2 and then separated by electrophoresis on DEAE-cellulose paper at pH 3.5 and 1,500 V for 3 h. The position of the cap structure was indicated on the electropherogram. Only the lower part of the electropherogram was exposed with an intensifying screen. The 70S RNA of Rous sarcoma virus (RSV; Prague strain of subgroup B) similarly digested was included for comparison. XC, Xylene cyanol dye marker; U, UMP; G, GMP; A, AMP; C, CMP.*

similar studies with both fractions. We found that both had a cap structure (data not shown) similar to that of the total RNA, further confirming that the poly(A)− fraction represented the degradation product of the positive-stranded RNA.

Comparative oligonucleotide fingerprinting of different MHV strains. Several antigenically related but serologically separable MHV strains have been isolated independently from different mouse colonies (17). They differ in their pathogenicity and perhaps also in some biological properties. To study their genetic relationship and possibly to identify the genetic basis for their pathogenicity, we compared different pathogenic and nonpathogenic MHV strains by oligonucleotide fingerprinting. ^{32}P-labeled 60S RNA was digested with RNase T_1 and then separated by two-dimensional polyacrylamide gel electrophoresis. Fig. 3 shows the oligonucleotide fingerprints of several hepatotropic strains, MHV-1, MHV-2, MHV-3, and MHV-S, a neurotropic strain, JHM, and a nonpathogenic strain, A59. In general, these strains had quite distinct and apparently unrelated fingerprints, with the exception of MHV-3 and A59, which appeared very much related. Because we were particularly interested in understanding the genetic basis of viral pathogenesis, the fingerprint of each pathogenic strain was compared with that of A59. Because these fingerprints differed quite extensively, it was difficult to determine, without knowing their sequences, whether two oligonucleotides on different fingerprints were identical. Therefore, to determine the exact identity of each oligonucleotide shared between two strains, we mixed and analyzed by oligonucleotide fingerprinting the RNAs of A59 and other MHV strains (Fig. 4). These fingerprints were compared with the fingerprints of each individual RNA (Fig. 3). If two oligonucleotides from two MHV strains were identical, they would comigrate as a single spot in the fingerprints of the RNA mixtures. Such analysis allowed us to determine the identity or nonidentity of each oligonucleotide spot in different MHV strains. This analysis is shown in Fig. 5. It can be seen that all of the pathogenic strains, with the exception of strain MHV-3 (Fig. 6), diverged quite extensively from strain A59. However, they also shared many large oligonucleotides identifiable in these fingerprints. Because the smaller oligonucleotides were likely not to be unique in their sequences, we studied only

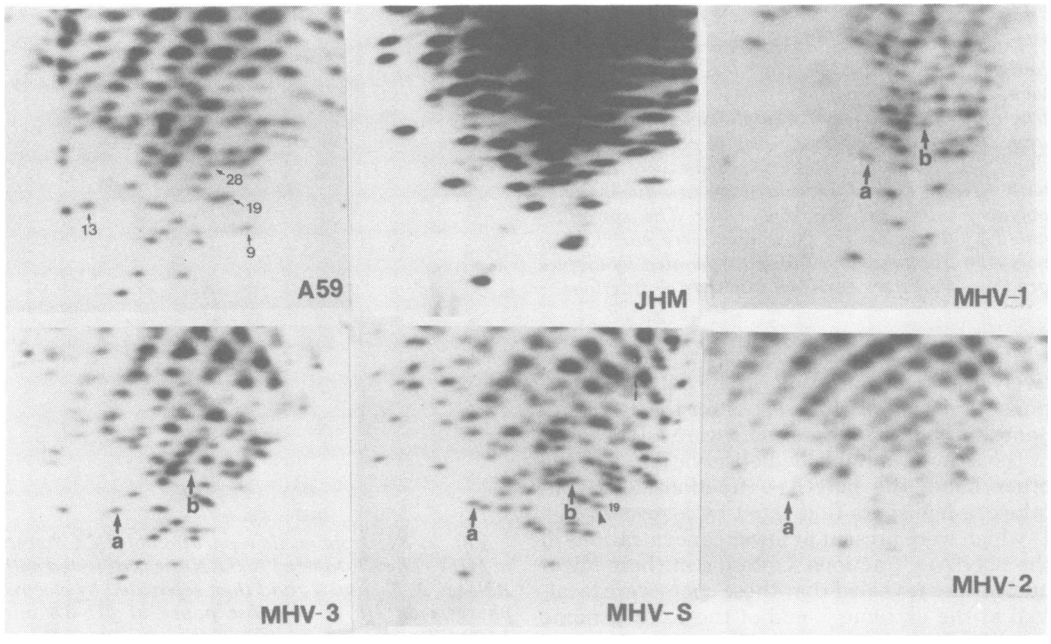

FIG. 3. *Oligonucleotide fingerprints of the genomic RNAs of different MHV strains. The ^{32}P-labeled 60S MHV RNAs were digested with RNase T_1 and separated by two-dimensional polyacrylamide gel electrophoresis. The spots indicated by arrows are the oligonucleotides that were shared with the MHV-3-specific spots (a and b) (see text), and the spots indicated by triangles are the oligonucleotides that were shared with the A59-specific oligonucleotides (no. 9, 13, 19, and 28) (see Fig. 4 to 6 for comparison). The numbering of oligonucleotides in A59 was arbitrary.*

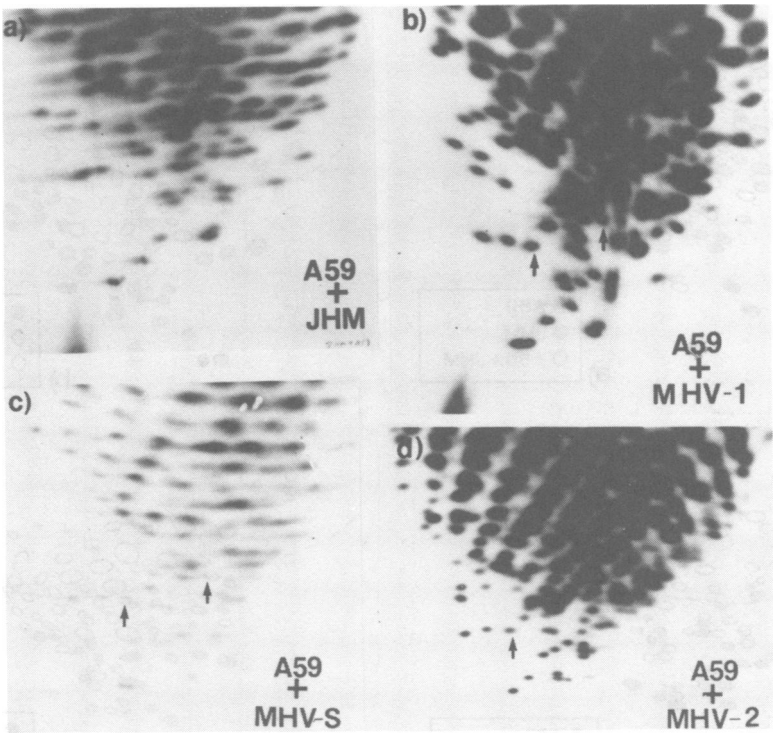

FIG. 4. *Oligonucleotide fingerprints of the RNA mixtures of A59 and other MHV strains. Equal amounts of ^{32}P-labeled 60S RNAs of A59 and JHM (a), MHV-1 (b), MHV-S (c), and MHV-2 (d) were mixed and digested with RNase T_1 and separated by two-dimensional polyacrylamide gel electrophoresis as for Fig. 1. The spots denoted by arrows are those that were identical to the MHV-3-specific spots a and b (see text).*

large oligonucleotides (the spots below the dashed lines in Fig. 5) as a basis for the comparison of different MHV strains. As shown in Fig. 5a, of the 60 large oligonucleotides of the neurotropic strain, JHM, 36 were shared with strain A59. If we assume that these large oligonucleotides were representative of the entire genomic sequences, then 60% of the JHM sequences were shared with A59. However, this figure is not necessarily accurate because only about 15% of the entire RNA sequences were represented in these large oligonucleotides. Therefore, this number can only be considered as an estimate. We performed the same kind of analysis for all MHV strains, taking into account the same reservations. The number of large T_1-oligonucleotides studied was lower for the virus strains which were more diverged, e.g., A59 and MHV-1 (Fig. 4b), because the higher complexity of the oligonucleotide patterns of these RNA mixtures made unequivocal identification of oligonucleotides impossible (Table 1). These analyses suggest that all of the pathogenic strains, with the exception of MHV-3, are related to A59 to the extent of 39 to 60% of the genomic sequences (Table 1). We conclude that all of these MHV strains diverged quite extensively. Similar conclusions can be drawn from a comparison of different pathogenic strains. About the same degree of homology (number of shared oligonucleotides) could be detected among various pathogenic MHV strains when their fingerprints were compared (data not shown). The only exception was seen in the comparisons of MHV-3 and A59, which appeared to share extensive sequence homology (Fig. 6).

Characterization of MHV-3 and A59-specific oligonucleotides. Strains MHV-3 and A59 are antigenically related but distinct (11; J. C. Childs and S. A. Stohlman, unpublished observations). They have identical profiles of virion structural proteins with similar molecular weights (see below). However, they differ in their pathogenicity: MHV-3 causes fulminating hepatitis in most strains of mice (16, 34; S. A. Stohlman, unpublished observation) and chronic choroidoependymitis and meningitis in a few strains of mice (29), whereas A59, employed in this study (see Materials and Methods), has very weak pathogenicity (19). Because A59 and MHV-3 had almost identical T_1-oligonucleotide fingerprints, it is possible that some

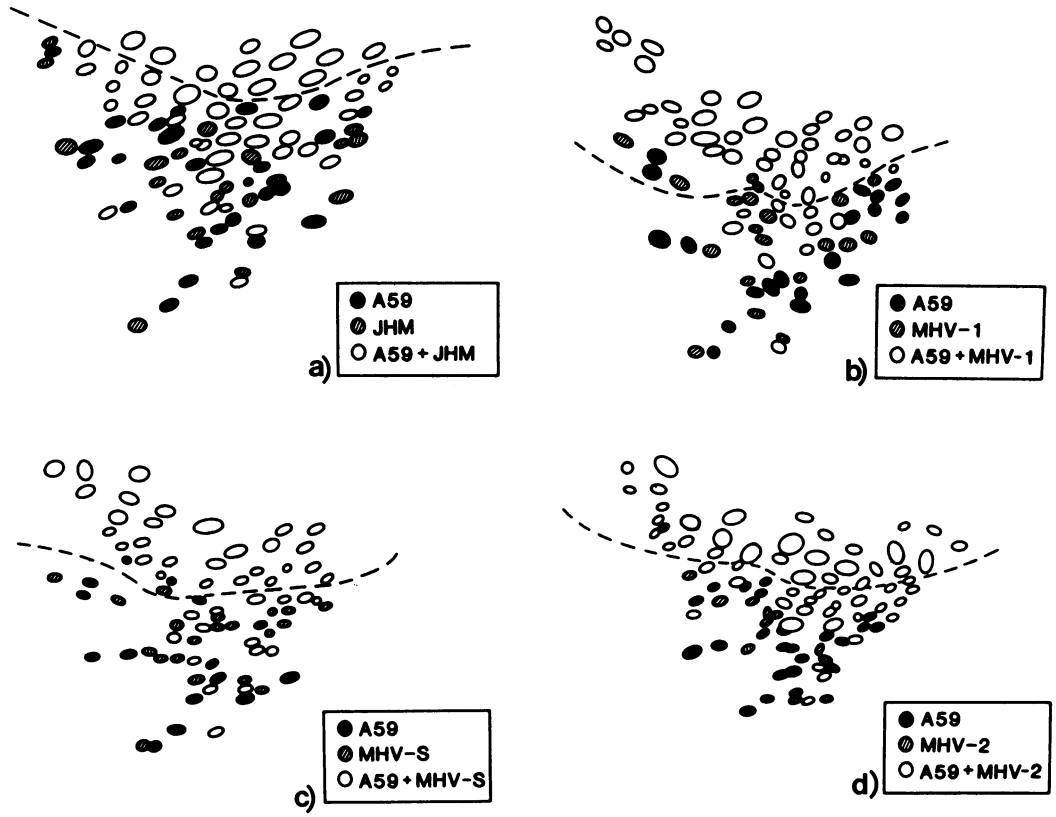

FIG. 5. *Schematic drawings of the oligonucleotide fingerprints of the RNA mixtures of A59 and other MHV strains. The data were obtained by comparing Fig. 4 with fingerprints of individual RNAs shown in Fig. 3. The solid spots are those that were specific for A59, the shaded spots are those that were specific for various pathogenic MHVs, and the open spots are those that were shared by A59 and other MHV strains. Parts (a), (b), (c), and (d) are as described in the legend to Fig. 4.*

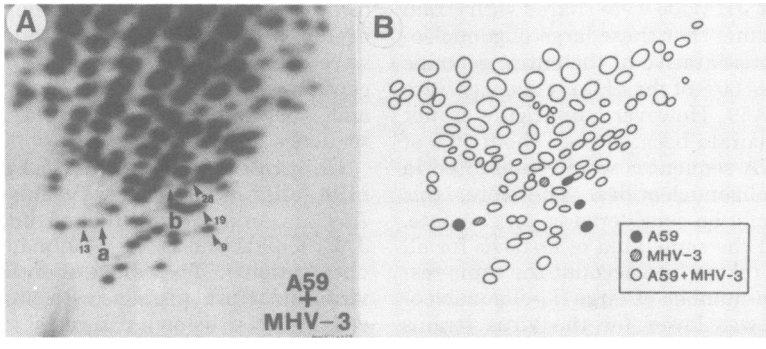

FIG. 6. *Oligonucleotide fingerprints of MHV-3 and A59. (A) Mixture of A59 and MHV-3; (B) schematic drawing of (A). The solid spots are those that were specific for A59, the shaded spots are those that were specific for MHV-3, and the open spots are those that were shared by A59 and MHV-3. The numbering of oligonucleotides was as described in the legend to Fig. 4. Only the A59- or MHV-3-unique spots are numbered.*

or all of the differences might be derived from the genetic sequences associated with the pathogenic or other biological properties of the virus. We therefore studied MHV-3 and A59 fingerprints in further detail. As shown in Fig. 6 and Table 1, MHV-3 and A59 shared 96 out of 100 identifiable T_1-oligonucleotides. However, MHV-3 had two specific oligonucleotides, designated a and b, and A59 had four specific oligonucleotides, designated no. 9, 13, 19, and 28,

TABLE 1. *Sequence relationship between A59 and other MHV strains*

Strain	No. (%) of A59 oligonucleotide spots shared[a]
JHM	36/60[b] (60)
MHV-1	11/28 (39)
MHV-2	26/46 (56)
MHV-3	96/100 (96)
MHV-S	15/28 (53)

[a] Only the large T_1-oligonucleotides shown below the dashed lines in each fingerprint shown in Fig. 5 and 6 were considered.

[b] The denominator represents the total number of T_1-oligonucleotides of A59 used for comparison.

which were not shared with each other (the numbers of oligonucleotides were arbitrarily assigned for every oligonucleotide in A59). Among these specific oligonucleotides, spot b of MHV-3 and spot no. 28 of A59 appeared to be present at a lower molar ratio than other spots. Mapping of these two oligonucleotides on the RNA genomes showed that these two spots were localized at the extreme 5′ end of their respective RNA genomes (unpublished observation). Therefore, their lower molar yield was probably due to degradation of the RNA genome during preparation. If these oligonucleotides were indeed localized in the genetic region either directly or indirectly associated with viral pathogenicity, then the MHV-3-specific oligonucleotides might be present in all of the MHV strains having similar pathogenicity. In contrast, the oligonucleotides specific for A59 should not be present in pathogenic strains. To test this possibility, we examined all MHV strains for the presence of these A59- or MHV-3-specific oligonucleotides. The identity of oligonucleotides was determined by comparing the electrophoretic mobility of these oligonucleotides in different MHVs and in A59 (Fig. 3 to 6) and also by comigration of the spots in the RNA mixture of MHV-3 and other MHV strains (data not shown). It was found that one of the MHV-3-specific oligonucleotide spots, a, was present in all four hepatotropic strains, but not in the oligonucleotide fingerprints of A59 or JHM, both of which cause minimal hepatitis (Table 2). The other spot, b, was present in MHV-1, MHV-3, and MHV-S, but not in MHV-2, A59, or JHM (Table 2). Therefore, these spots, particularly spot a, appear to be conserved in, and unique to, most of the hepatotropic strains. On the other hand, among the four A59-specific oligonucleotides, spot no. 19 was also present in MHV-S, a hepatotropic strain of reduced virulence (27). Spot no. 9 was occasionally seen in some preparations of MHV-3 RNA; therefore, it is probably not a real A59-specific oligonucleotide. Thus, only spot no. 13 and spot no. 28 are unique to nonpathogenic A59.

Comparison of viral structural proteins of different MVH strains. RNase T_1-oligonucleotide fingerprinting analysis of MHV RNA suggested that different MHV strains diverged quite extensively, whereas A59 and MHV-3 were very much related. To study the genetic localization of the sequence heterogeneity and homology among these MHV strains, we compared their structural proteins to see whether the size and structure of these proteins reflected their sequence relatedness. ^{3}H-amino acid-labeled viral proteins were separated by electrophoresis on 6 to 18% gradient polyacrylamide gels. As shown in Fig. 7A, all of the MHV strains contained structural proteins of similar molecular weight. But there were some minor variations. Particularly noteworthy was that the $pp50^{NP}$'s (23) of A59 and MHV-3 had molecular weights slightly lower than those of other MHV strains. This difference was reproducible and could best be seen in 10% polyacrylamide gel electrophoresis (Fig. 7B). There was no difference in the migration rate between the $pp50^{NP}$'s of MHV-3 and of A59. Thus, consistent with the results of oligonucleotide fingerprinting, these data suggest that MHV-3 is more closely related to A59 than other MHV strains are. Among other strains there was no detectable difference in the molecular weight of $pp50^{NP}$. However, MHV-S had an additional protein, p65 (Fig. 7A), which was not seen in other strains. Whether this represented an isomer of pp50 or a cellular contaminant is being investigated. Between MHV-3 and A59 there appeared to be a slight difference in the electrophoretic mobility of gp180 (Fig. 7A). It was not clear, however, whether this difference reflected a real difference in the molecular weight of the protein moiety or was due to a difference in the glycosylation of the protein. Also, it was not clear whether this difference corresponded to the sequence divergence between the RNA genomes of these two strains. There were also a few more minor protein bands

TABLE 2. *Distribution of MHV-3- and A59-specific oligonucleotides in different MHV strains*

Strain	Distribution[a] of the following spots					
	a	b	13	28	19	9
MHV-3	+	+	−	−	−	±
MHV-1	+	+	−	−	−	−
MHV-2	+	−	−	−	−	−
MHV-S	+	+	−	−	+	−
A59	−	−	+	+	+	+
JHM	−	−	−	−	−	−

[a] Data were obtained from Fig. 3 to 6. +, Present; −, absent.

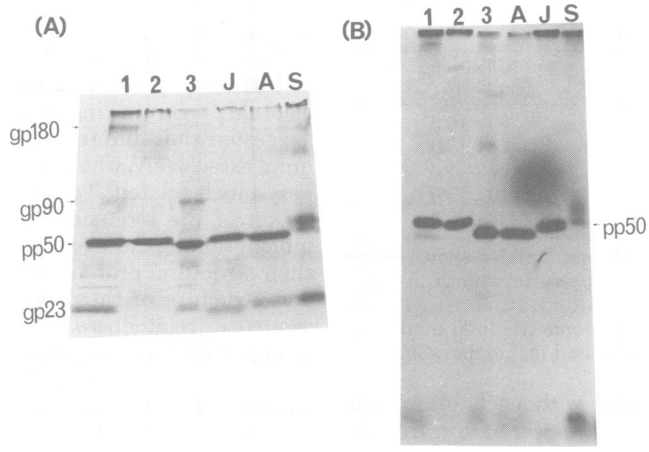

FIG. 7. *Polyacrylamide gel electrophoresis of viral structural proteins. ^{3}H-amino acid-labeled viral proteins from different MHV strains were separated by electrophoresis on a 6 to 18% linear gradient (A) or 10% fixed concentration polyacrylamide gel (B). Virion structural proteins from vesicular stomatitis virus were used as molecular weight markers. 1, MHV-1; 2, MHV-2; 3, MHV-3; S, MHV-S; A, A59; and J, JHM.*

in several MHV strains. These proteins could represent cellular contaminants or aggregates of viral proteins. Such minor proteins have occasionally been observed previously in some MHV strains (32).

DISCUSSION

Our studies have concluded that the MHV genome is a positive-stranded, single-stranded 60S RNA. No negative-stranded RNA could be detected in the viral particles. Because MHV is an enveloped RNA virus with helical nucleocapsid (18), coronavirus becomes the first virus with such characteristics to possess a positive-stranded RNA genome. All other RNA virus groups with helical nucleocapsids, including myxoviruses, paramyxoviruses, and rhabdoviruses, have negative-stranded RNA genomes. Although Newcastle disease virus and Sendai virus also contain some positive-stranded RNA in the viral particles (20), their viral genomes have been clearly shown to be negative stranded. The significance of the poly(A)-lacking 60S RNA species present in the MHV particles is not clear. They appear to represent the degradation products of the positive-stranded RNA genome.

The comparative analyses of oligonucleotide fingerprints of different MHVs independently isolated from different mouse colonies suggest that they have diverged quite extensively. However, the exact degree of homology or divergence could not be determined by our technique because the large T_1-oligonucleotides we analyzed represent at most 15 to 20% of the entire genomic sequences. Also, some of the oligonucleotides which comigrated in two-dimensional polyacrylamide gels might represent isomers rather than identical sequences. Therefore, the data presented in Table 1 can only be interpreted to indicate that the different MHV strains are quite heterogeneous. Direct comparison of these strains for the purpose of studying the mechanism of viral pathogenesis is, therefore, not useful, because these strains have diverged too extensively in their genetic sequences. Rather, two strains which are closely related but differ in pathogenicity should be selected for this purpose. The oligonucleotide fingerprinting will then be useful in localizing genetic differences between these closely related or congenic virus strains. We found that MHV-3 and A59 could represent such a virus pair.

MHV-3 and A59 were independently isolated from different mouse colonies. Their antigenic properties are related but distinct (11; J. C. Childs and S. A. Stohlman, unpublished observations). Their structural proteins are very closely related (Fig. 7), and their in vitro biological characteristics also appear to be quite similar. However, in experimental animals, MHV-3 is strongly pathogenic (16, 34; S. A. Stohlman, unpublished observation), whereas A59, used in this study, is not (19). Because we found that these two strains extensively shared their oligonucleotides, it is possible that at least some of the oligonucleotides specific for MHV-3 or A59 could have come from the genetic region directly or indirectly associated with viral pathogenicity. It was noted from our analysis that one of the two MHV-3-specific spots, a, was shared with all of the hepatotropic strains, whereas the other

spot, b, was present in only three hepatotropic strains, but not in MHV-2. It is interesting to note that MHV-2 is different from other MHV strains in that it does not induce syncytia formation in vitro (12; S. A. Stohlman, unpublished observations). Thus, the genetic region corresponding to spot b might be related to other biological properties of MHV. On the other hand, among the A59-specific spots, only spot no. 13 and spot no. 28 were absent in the fingerprints of all of the hepatotropic strains. Spot no. 19 was present also in MHV-S, which has lower hepatotropic capacity (27). Therefore, spot b of MHV-3 and spot. no. 13 and spot no. 28 of A59 have perfect correlation with viral pathogenicity. Preliminary data showed that spot b and spot no. 28 were localized at the same position at the 5′ end of the genomes, whereas spot a and spot no. 13 were mapped at the same position at 6 to 7 kilobases from the 3′ end of the genomes of MHV-3 and A59, respectively (unpublished observation). Thus, spot a, and spot no. 28 and spot b and spot no. 13 might represent mutations of the same genetic sequences in MHV-3 and A59, respectively. The biological significance of these two genetic regions remains to be studied. Although it is tempting to suggest that these regions might be directly or indirectly associated with viral hepatotropic properties, additional strains need to be investigated before their functions can be firmly established. It is interesting to note that MHV-3 and A59 differ slightly in the molecular weights of their gp180's (Fig. 7A). Whether this envelope glycoprotein represents the gene product of one of these genetic regions is not clear at the present time.

This approach represents our first attempts at understanding the molecular basis of MHV-induced pathogenicity. The difficulty in this approach is the lack of congenic virus mutants or variants which have single mutations and thus allow unequivocal demonstration of the genetic region(s) associated with pathogenicity. It remains to be elucidated whether MHV-3 and A59 fulfill such a requirement, i.e., if they are homologous for all of the genetic sequences except for the region directly associated with viral pathogenicity. More definitive studies will have to be performed with laboratory-derived virus mutants. Preliminary data in our laboratories suggest that it is possible to obtain such virus variants. We have analyzed two congenic JHM variants which differ only in their demyelinating capacity in vivo and plaque morphology in vitro. As expected, their oligonucleotide fingerprints differ only very slightly. Such variants will allow us to determine more directly the genetic regions responsible for viral pathogenicity. Such experiments are in progress.

ACKNOWLEDGMENTS

We thank Chris Patton, Cynthia Yung, and Thomas Hanson for excellent technical help and Josie Lopez for editorial assistance.

This work was supported in part by grant PCM-7904567 from the National Science Foundation and by Public Health Service grants NS12967, NS15079, and CA 16113 from the National Institutes of Health.

LITERATURE CITED

1. **Aviv, H., and P. Leder.** 1972. Purification of biologically active globin messenger RNA by chromatography in oligo thymidylic acid-cellulose. Proc. Natl. Acad. Sci. U.S.A. **69**:1408–1412.
2. **Bailey, O. T., A. M. Pappenheimer, F. S. Cheever, and J. B. Daniels.** 1949. A murine virus (JHM) causing disseminated encephalomyelitis with extensive destruction of myelin. II. Pathology. J. Exp. Med. **90**:195–212.
3. **Bonner, W. M., and R. A. Lasky.** 1974. A film detection method for tritium-labeled proteins and nucleic acids in polyacrylamide gels. Eur. J. Biochem. **46**:83–88.
4. **Calisher, C. H., and W. P. Rowe.** 1966. Mouse hepatitis, Reo-3 and Theiler viruses. Natl. Cancer Inst. Monogr. **20**:67–75.
5. **Cheever, L. S., J. B. Daniels, A. M. Pappenheimer, and O. T. Bailey.** 1949. A murine virus (JHM) causing disseminated encephalomyelitis with extensive destruction of myelin. I. Isolation and biological properties of the virus. J. Exp. Med. **90**:181–194.
6. **deWatcher, R., and W. Fiers.** 1972. Preparative two dimensional polyacrylamide gel electrophoresis of ^{32}P-labeled RNA. Anal. Biochem. **49**:184–197.
7. **Dick, G. W., J. Niven, and A. Gledhill.** 1956. A virus related to that causing hepatitis in mice (MHV). Br. J. Exp. Pathol. **37**:90–96.
8. **Furuich, Y., and K. Miura.** 1975. A blocked structure at the 5′ terminus of mRNA from cytoplasmic polyhedrosis virus. Nature (London) **253**:374–375.
9. **Gledhill, A., and O. C. Andrews.** 1951. A hepatitis virus of mice. Br. J. Exp. Pathol. **32**:559–568.
10. **Herndon, R. M., D. E. Griffin, U. McCormick, and L. P. Weiner.** 1975. Mouse hepatitis virus-induced recurrent demyelination. Arch. Neurol. **32**:32–35.
11. **Hierholzer, J. C., J. R. Broderson, and F. A. Murphy.** 1979. New strain of mouse hepatitis virus as the cause of lethal enteritis in infant mice. Infect. Immun. **24**: 508–522.
12. **Hirano, N., K. Kujiwara, S. Hino, and M. Matumoto.** 1974. Replication and plaque formation of mouse hepatitis virus (MHV-2) in mouse cell line DBT culture. Arch. Virol. **44**:298–302.
13. **Keith, J., and H. Fraenkel-Conrat.** 1975. Identification of the 5′ end of Rous sarcoma virus RNA. Proc. Natl. Acad. Sci. U.S.A. **72**:3347–3358.
14. **Laemmli, U. K.** 1970. Cleavage of structural proteins during assembly of the head of bacteriophage T4. Nature (London) **227**:680–685.
15. **Lai, M. M. C., and S. A. Stohlman.** 1978. RNA of mouse hepatitis virus. J. Virol. **26**:236–242.
16. **Macnaughton, M., and S. Peterson.** 1980. Mouse hepatitis virus strain 3 infection of C57, ASn and AJ strain mice and their macrophages. Arch. Virol. **66**:71–75.
17. **McIntosh, K.** 1973. Coronaviruses: a comparative review. Curr. Top. Microbiol. Immunol. **63**:85–129.
18. **Oshiro, L. S.** 1973. Coronaviruses, p. 331–343. *In* A. J. Dalton and F. Haguenau (ed.), Ultrastructure of animal viruses and bacteriophages: an atlas. Academic Press, Inc., New York.
19. **Robb, J. A., and C. W. Bond.** 1979. Pathogenic murine coronaviruses. I. Characterization of the biological behavior *in vitro* and virus-specific intracellular RNA of strongly neurotropic JHMV and weakly neurotropic A59V viruses. Virology **94**:352–370.

20. **Robinson, W. S.** 1970. Self-annealing of subgroup 2 myxovirus RNAs. Nature (London) **225**:944–946.
21. **Rowe, W., J. Hartley, and W. Capps.** 1963. Mouse hepatitis virus infection as a highly contagious, prevalent enteric infection of mice. Proc. Soc. Exp. Biol. Med. **112**:161–165.
22. **Shatkin, A. J.** 1974. Methylated messenger RNA synthesis in vitro by purified reovirus. Proc. Natl. Acad. Sci. U.S.A. **71**:3204–3207.
23. **Stohlman, S. A., and M. M. C. Lai.** 1979. Phosphoproteins of murine coronaviruses. J. Virol. **32**:672–675.
24. **Stohlman, S. A., and L. P. Weiner.** 1981. Chronic central nervous system demyelination in mice with a defective JHM virus infection. Neurology **31**:38–44.
25. **Sturman, L. S., and K. K. Takemoto.** 1972. Enhanced growth of a murine coronavirus in transformed mouse cells. Infect. Immun. **6**:501–507.
26. **Taguchi, F., N. Hirano, Y. Kiuchi, and K. Fujiwara.** 1976. Difference in response to mouse hepatitis virus among susceptible mouse strains. Jpn. J. Microbiol. **20**: 293–302.
27. **Taguchi, F., A. Yamada, and K. Fujiwara.** 1979. Factors involved in the age-dependent resistance of mice infected with low-virulence mouse hepatitis virus. Arch. Virol. **62**:333–334.
28. **Tyrrell, D. A. J., D. J. Almeida, C. H. Cunningham, B. C. Easterday, D. J. Garwes, J. C. Hierholzer, A, Kapikian, M. R. MacNaughton, and K. McIntosh.** 1978. Coronaviridae: second report. Intervirology **10**: 321–328.
29. **Virelizier, J. L., A. D. Dayan, and A. C. Allison.** 1975. Neuropathological effects of persistent infection of mice by mouse hepatitis virus. Infect. Immun. **12**:1127–1140.
30. **Wang, L. H., P. H. Duesberg, T. Robins, H. Yokota, and P. K. Vogt.** 1977. The terminal oligonucleotides of avian tumor virus RNAs are genetically linked. Virology **82**:472–492.
31. **Wege, H., A. Muller, and V. ter Meulen.** 1978. Genomic RNA of the murine coronavirus JHM. J. Gen. Virol. **41**:217–228.
32. **Wege, H., H. Wege, K. Nagashima, and V. ter Meulen.** 1979. Structural polypeptides of the murine coronavirus JHM. J. Gen. Virol. **42**:37–47.
33. **Weiner, L. P.** 1973. Pathogenesis of demyelination induced by a mouse hepatitis virus (JHM virus). Arch. Neurol. **28**:298–303.
34. **Yamada, A., F. Taguchi, and K. Fujiwara.** 1979. T-lymphocyte-dependent difference in susceptibility between DDD and C3H mice to mouse hepatitis virus, MHV-3. Jpn. J. Exp. Med. **49**:413–421.